Int J Clin Exp Pathol 2021;14(1):86-96
www.ijcep.com /ISSN:1936-2625/IJCEP0120242

Original Article

miR-133b has protective effect on rats with acute lung injury caused by severe acute pancreatitis through targeting sp1 gene

Yunqi Weng, Nan Lin, Lei Yin, Aiguo Liu

Department of Emergency, The Affiliated Hospital of Qingdao University, Qingdao, Shandong Province, China

Received August 13, 2020; Accepted November 16, 2020; Epub January 1, 2021; Published January 15, 2021

Abstract: Objective: We aimed to investigate the regulatory mechanism of miR-133b and Sp1 in rats with severe acute pancreatitis complicated by acute lung injury. Methods: The rats were divided into normal, NC, model, si-Sp1, miR-133b mimic, miR-133b inhibitor, and miR-133b inhibitor + si-Sp1 group and received different treatments. Results: Compared with normal mice, model mice had a lower miR-133b expression, but higher levels of Sp1 expression, W/D of lung tissue, myeloperoxidase activities, and higher levels of interleukin(IL)-6, tumor necrosis factor (TNF)-α and IL-1β, cell apoptosis rate and Notch-1, and Hes-1, nuclear factor (NF)-κB P65 expressions in lung tissue. Compared with model mice, mice in the si-Sp1 group and the miR-133b mimic group had significantly lower W/D of lung tissue, myeloperoxidase activities, lower levels of IL-6, TNF-α and IL-1β, cell apoptosis rate and Notch-1, Hes-1, and NF-κB P65 expressions in lung tissue. Mice treated by miR-133b inhibitor showed opposite results in all above parameters, which were similar with those in the model group. The negative effects of miR-133b inhibitor could be reversed by the combination use of si-Sp1. Conclusion: Overexpression of miR-133b could inhibit Sp1 expression, thereby improving severe acute pancreatitis in rats and playing a protective role in acute lung injury.

Keywords: miR-133b, acute pancreatitis, acute lung injury

Introduction

Severe pancreatitis-related acute lung injury (PALI) is a common, but serious complication of severe acute pancreatitis (SAP), which is also one of the main causes of early death in patients with SAP [1]. In SAP, the damaged lung tissues recruit immune cells and release cytokines, chemokines, growth factors, and prostaglandins, to promote acute inflammatory responses [2]. To reveal the pathogenesis of this disease, a variety of animal models have been developed and studied previously [3-5]. In general, systemic inflammation is considered to be a prerequisite for the pathogenesis of SAP-induced acute lung injury (ALI), which is characterized by immune cell infiltration of the lungs, local and systemic release of proinflammatory mediators, and activation of various inflammatory pathways [6]. Although significant progress has been made in explaining this disease, a comprehensive molecular explanation is still elusive and hence developing a specific treatment has been difficult.

MicroRNA (miRNA) is one type of small non-coding RNA containing 22 nucleotides [7]. They can regulate gene expression by binding with the mRNA of target gene and play a variety of roles in many cellular processes. Overexpression or reduced expression of miRNAs is involved in the pathophysiology of various disorders [8]. The discovery of miRNA dysregulation not only broadens our biological understanding of diseases, but may also provide a new class of markers. Evidence suggests that miRNAs may be potential biomarkers of pancreatic injury [9, 10]. For example, miR-127 was found to be in low expression levels in plasma of patients with SAP [9]. A recent study has also found that miR-133b can improve functional recovery after spinal cord injury in mice [10]. The mechanism of action of miR-133b in PALI has not been elucidated.

SPI/KLsF is a highly-related zinc finger protein involved in the transcription process in eukaryotic cells. It regulates important cellular functions such as cell proliferation, apoptosis, dif-

ferentiation, and tumor formation by regulating the GC-rich promoter gene expression in a cell- and promoter-specific manner [11]. It is now known that Sp1 is also associated with the regulation of signaling pathway genes and the process of tissue-specific cell cycle [12]. Sp1 is a member of the specific protein/Kruppel-like factor (Sp/KLF) transcription factor family and contains 26 proteins [13]. Sp1 is related to the basic transcriptional mechanism by interacting with TATA binding protein (TBP) and various TBP-related factors [14]. The role of Sp1 in SAP, complicated by ALI, in rats is not known.

Notch family is an important transmembrane signaling receptor proteins, and is involved in regulating cell proliferation and apoptosis in normal physiology. Notch/Hes signal pathway also regulates apoptosis in inflammatory cells [15]. It has been confirmed that this signaling pathway plays an important role in the differentiation of T and B lymphocytes [16]. Nuclear factor kappa-binding (NF-κB) can initiate the gene expression of many inflammatory mediators and is the key link in the initiation of an inflammatory reaction [17]. We speculated whether acute pancreatitis, complicated with ALI, is related to factors such as Notch-1, Hes-1, and NF-κB P65. Through bioinformatics predictions, a targeted relationship between miR-133b and Sp1 was confirmed. The level of miR-133b was inhibited in mice with spinal cord injury. We speculated that miR-133b may improve SAP, complicated with ALI, in rats by targeting to Sp1 to down-regulate the expression of Sp1.

In this study, we established a SAP rat model, complicated with ALI, to evaluate whether miR-133b can improve the SAP, complicated with ALI, in rats by targeting and down-regulating the expression of Sp1.

Material and methods

Experimental subjects

Seventy healthy clean-grade male SD rats, aged 2 weeks and weighing 200-220 g, were divided into the normal control group (normal group, n=10) and the SAP, complicated by ALI, group (model group, n=60). Food and tap water were freely available for rats. The establishment of model rats was performed according to the previous report [18]. A retrograde injection of 4% sodium taurocholate was applied into the pancreatic bile tract, the rats were fixed on the operating table after anesthesia, and the abdominal cavity was exposed. An incision was made on the abdomen. After dissociating the pancreatic duodenum in the medial duodenum, the pancreatic bile tract was clamped with a non-invasive metal clip. A 4.5# needle was retrogradely entered into the pancreatic bile tract 2 mm from the duodenal wall, after which the tract at the duodenal side was clamped with a non-invasive metal clip. Meanwhile, 4% sodium taurocholate (1 mL/kg) was continuously injected into the pancreatic duct through the duct wall for 1 min. The needle was kept in situ for 5 minutes, and both ends of the metal clip were loosened. The SAP model was successfully established when the significant edema and bleeding under the pancreatic capsule were confirmed. Four animals were not successfully modeled, with a successful rate of modeling of 95%. All animal experiment procedures were approved by the Ethics Committee of The Affiliated Hospital of Qingdao University, and strictly carried out in accordance with the Helsinki Declaration.

Grouping and processing

The mice were divided into 7 groups for experimental treatment: the normal group, the model group, the NC group, the miR-133b inhibitor group, the si-Sp1 group, and the miR-133b inhibitor + si-Sp1 group. The NC sequence, miR-133b mimic, miR-133b inhibitor, and si-Sp1 sequence adenoviral vectors were constructed by Tianjin Saier Biotechnology Co., Ltd., NC, miR-133b mimic, and miR-133b inhibitor were constructed using pWPI. si-Sp1 was constructed using the pSilencer 2.1-U6 vector. Rats were laid in a supine position on the operating table with the limbs fixed. The 5 μg of virus was injected into the abdominal cavity of the rats once a week. After 3 weeks of continuous injection, blood was collected from the orbital vein of the eyeball. Then mice were sacrificed to collect lung tissue samples [19]. The lung tissues and venous blood collected from five rats were used for detection. Part of the lung tissues were fixed in 10% neutral formalin solution. After 24 hours, the gradient alcohol was used to dehydrate the tissues, and then they were embedded in paraffin. The remaining tissues were stored in liquid nitrogen for later analysis.

Table 1. qRT-PCR primer sequence

Name	Sequence
miR-133b	F: 5'-GGGTTTGGTCCCCTTCA-3'
	R: 5'-CAGTGCGTGTCGTGGAGT-3'
Sp1	F: 5'-AGGTGCACCAGCTTCCAGGCCTG-3'
	R: 5'-CCAGGTCCATGAAGGCCAAGT-3'
Notch-1	F: 5'-CACCCATGACCACTACCCAGTT-3'
	R: 5'-CCTCGGACC AATCAGAGATGTT-3'
Hes-1	F: 5'-ACTGCATGACCCAGATCAACGC-3'
	R: 5'-GGAAGGCGACACTGCGTTAGGA-3'
NF-κB P65	F: 5'-TGCACCTAGCTGCCAAAGAAGGA-3'
	R: 5'-TCTGCTCCTGCTGCTTTGAGAA-3'
U6	F: 5'-GCTTCGGCAGCACATATACTAAAAT-3'
	R: 5'-GCACTCCCGCCACAAAGATG-3'
GAPDH	F: 5'-GGGAAATTCAACGGCACAGT-3'
	R: 5'-AGATGGTGATGGGCTTCCC-3'

Note: F: forward; NF-κB: nuclear factor kappa-binding; R: reverse; GAPDH: glyceraldehyde-3-phosphate dehydrogenase.

Dual luciferase reporter assay

The binding site of miR-133b and Sp1 was analyzed by the biological prediction tool (www.targetscan.org). The targeting relationship between miR-133b and Sp1 was confirmed by the dual luciferase reporter gene system assay. The dual luciferase reporter vector of the target gene Sp1 and the mutant of the miR-133b binding site were constructed respectively: PGL3-Sp1 wt and PGL3-Sp1 mut. Rellina plasmid and two reporter plasmids were co-transfected with miR-133b plasmid and NC plasmid into HEK293T cells. Dual luciferase assays were performed 24 hours post cell transfection. The cells in each group were first lysed, and then centrifuged at 12,000× g for 1 min. The supernatant was collected and luciferase activity was assessed according to the kit instructions (Promega).

Quantitative real-time PCR

Total RNA was extracted with Trizol (Thermo Fisher Scientific, New York, USA; Harbin Xinhai Genetic Testing Co., Ltd., China). cDNA was synthesized by using TaqMan MicroRNA Assays Reverse Transcription Primer (Thermo Scientific, USA). SYBR® PremixExTaqTM II Kit (Xingzhi Biotechnology Co., Ltd., China) was used for quantitative PCR detection. The following agents were applied in sequence: 25 μL of SYBR® PremixExTaqTM II (2×), 2 μL each of PCR upstream and downstream primers, 1 μL of ROX Reference Dye (50×), 4 μL of DNA template, and 16 μL of ddH_2O. Fluorescence quantitative PCR was performed in ABIPRISM® 7300 (Shanghai Kunke Instrument and Equipment Co., Ltd., China). The reaction conditions were as follows: pre-denaturation at 95°C for 10 min, denaturation at 95°C for 15 s, and annealing at 60°C for 30 s. After 32 cycles, elongation was conducted at 72°C for 1 min. U6 was used as an internal reference for miR-186. GAPDH was used as internal references for other genes. The $2^{-\Delta\Delta Ct}$ was used to calculate the relative expression of each target gene. **Table 1** shows the primers below.

Western blot

Total protein was extracted using Radio Immunoprecipitation Assay lysate (R0010, Solarbio) containing Phenylmethanesulfonyl fluoride. The BCA kit (Thermo, Inc., USA) was used to measure the protein concentration. A total of 30 μg of protein sample was loaded and separated by electrophoresis at 80 V for 2 h followed by transferring onto a PVDF membrane (Millipore, Billerica, MA, USA) at a voltage of 110 V for 2 h. The proteins on the membrane were blocked by 5% skim milk at 4°C for 2 h. Then, the primary rabbit anti-mouse antibodies for Sp1 (ab16660, 1:25, Abcam, UK), Notch-1 (ab52627, 1:1,000, Abcam, UK), Hes-1 (ab71-559, 1:1,000, Abcam, UK), NF-κB P65 (ab32-536, 1:5,000, Abcam, UK), and GAPDH (ab8-226, 1:2,000, Abcam, UK) were added onto the membrane. The membrane was incubated with antibodies overnight at 4°C. The sample was incubated with HRP-labeled goat anti-rabbit IgG antibody (Beijing Zhongshan Biotechnology Co., Ltd., diluted with 1:5,000). After washing, ECL fluorescence detection kit (Amersham, UK) was used to develop the sample, which was imaged by Bio-Rad image analysis system (BIO-RAD, USA). The relative protein content was expressed by the gray value of the corresponding protein band/the gray value of the GAPDH protein band.

The measurement of Wet/dry weight ratio (W/D) of lung tissues

The left lung of the rat was collected by thoracotomy. The wet weight was detected after blotting blood and water on the lung surface

with filter paper. After drying in 80°C incubator for 48 h to a constant weight, the lung dry weight was also determined. The W/D and water content in the lung tissue were used to reflect the degree of edema in the lung, and was calculated as follows: wet/dry weight = wet weight/dry weight * 100%.

Myeloperoxidase (MPO) activity

The MPO activity was determined to measure the degree of neutrophil infiltration in lung tissues. The MPO colorimetric activity assay kit (Biovision, US) was used to measure MPO activity and the procedure was carried out according to the kit instructions.

ELISA

Venous blood was centrifuged at 12,000× g for 10 min. The serum was separated and stored at -20°C. The levels of cytokines interleukin (IL)-1β, tumor necrosis factor (TNF-α), and IL-6 were measured according to the instructions of ELISA kits (Wuhan Merck, China).

TUNEL assay

Paraffin sections were dewaxed and hydrated, then immersed and washed in 3% H_2O_2 for 12 min. Proteinase K (Solarbio, 20 μg/mL, dissolved in Tris/HCl) was added and it was incubated at room temperature for 30 min. These sections were washed with PBS 3 times, and the excess water was wiped off. The TUNEL reaction mixture was added onto sections dropwise. Sections were incubated in a humid chamber at 37°C for 1 h and then washed with PBS 3 times. The sections were observed using a fluorescence microscope (ECLIPSE Ti, Nikon, Japan). Brown-stained cells were considered TUNEL-positive cells. Three fields of view were randomly selected to calculate the percentage of TUNEL-positive cells from the total cells, namely the apoptotic index (AI).

Statistical analysis

All the data collected in this study were analyzed using SPSS 21.0 software. Measurement data were expressed as mean ± standard deviation. The differences among multiple groups were examined using one-way ANOVA. The pairwise comparisons of the mean values between multiple groups were tested by Tukey's post-hoc test. $P<0.05$ was considered statistically significant.

Results

MiR-133b targets and negatively regulates Sp1 gene in lung tissues of rat

Through the prediction of the bioinformatics website, the specific binding site between miR-133b and Sp1 is showed in **Figure 1A**. The results of dual luciferase reporter test showed (**Figure 1B**) that the luciferase activity of the wild-type Sp1 (Wt-Sp1) and miR-133b mimic co-transfected group was significantly lower than that in NC mimic co-transfected group ($P<0.05$). The luciferase activity of the mutant Sp1 (Mut-Sp1) plasmid group did not change significantly ($P>0.05$). Hence, miR-133b could be targeting and negatively regulating the level of Sp1 gene.

To evaluate how miR-133b targets Sp1 gene expression and protects rats from SAP, combined with ALI, we measured the expression of miR-133b and Sp1 mRNA by quantitative real-time PCR and quantified the expression of Sp1 protein by western blot. The results showed that (**Figure 1C-E**) when compared with the normal group, the miR-133b expression in other groups were significantly downregulated. The expression level of Sp1 was significantly upregulated ($P<0.05$). Compared with the model group, there was no significant difference in the expression of Sp1in the NC group and the miR-133b inhibitor + si-Sp1 group. The expression of Sp1 was significantly lower in the miR-133b mimic group and the si-Sp1 group. The expression of Sp1 in miR-133b inhibitor group was significantly higher ($P<0.05$). Compared with the miR-133b inhibitor group, the expression of Sp1 in the miR-133b mimic group, and the si-Sp1 group, as well as the miR-133b inhibitor + si-Sp1 group showed the significantly decreased. The level of miR-133b significantly increased in the miR-133b mimic group, but significantly decreased in the miR-133b inhibitor group and miR-133b inhibitor + si-Sp1 group (both $P<0.05$).

The W/D, MPO activity and IL-1β, IL-6 and TNF-α levels in venous blood of rats in each group

The W/D, MPO activity, IL-1β, IL-6, and TNF-α levels of the other groups were significantly

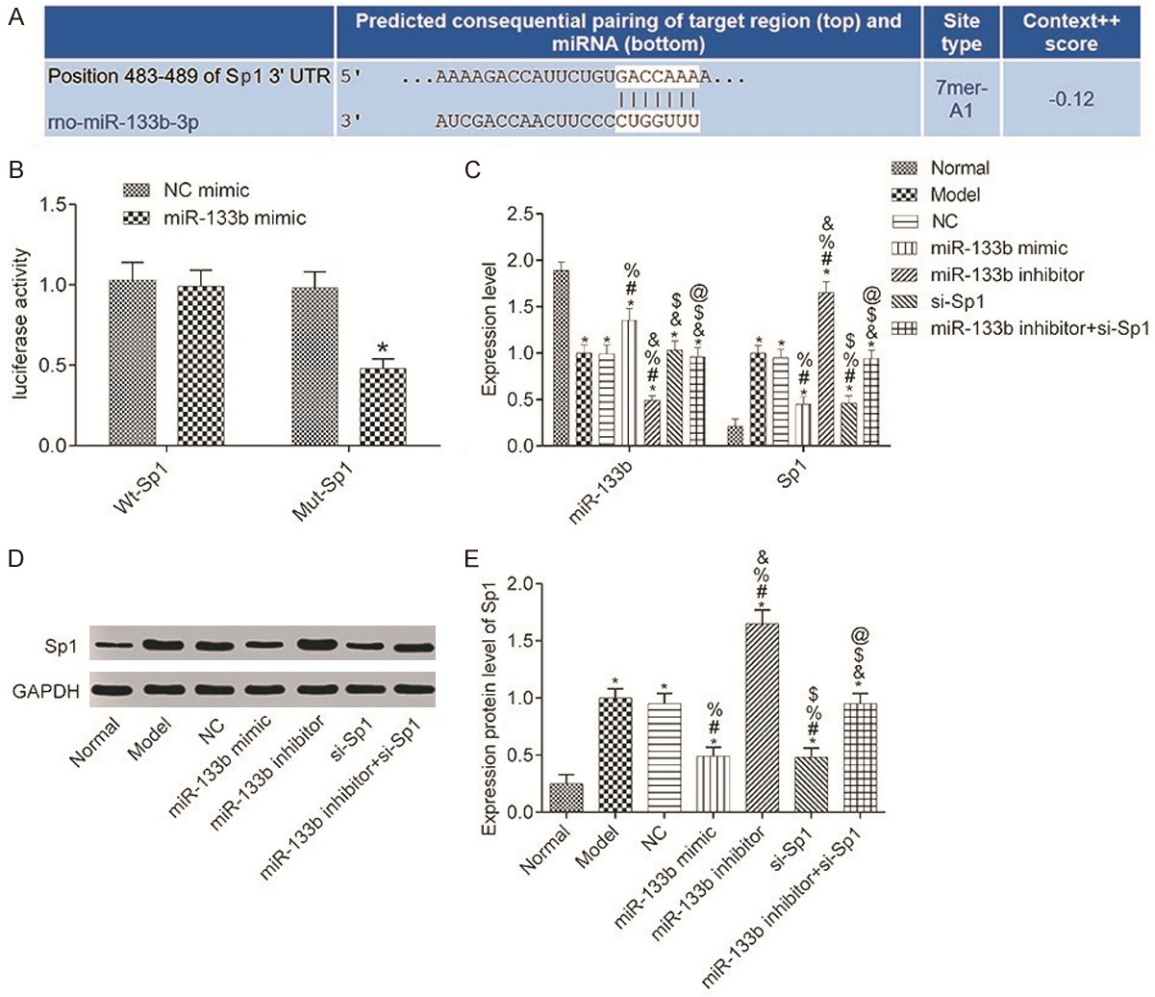

Figure 1. miR-133b targets and negatively regulates Sp1 gene in lung tissues of rat. A: 3'-UTR sequence region of miR-133b binding to Sp1; B: The double luciferase reporter system assay; C: miR-133b and Sp1 expression level; D: Protein bands; E: Expression protein level of Sp1. Compared with normal group, *P<0.05; compared with model group, $^{\#}$P<0.05; compared with NC group, $^{\%}$P<0.05; compared with miR-133b mimic group, $^{\&}$P<0.05; compared with miR-133b inhibitor group, $^{\$}$P<0.05; compared with si-Sp1 group, $^{@}$P<0.05. NC, negative control.

higher than those of the normal group (P< 0.05). There were no significant differences in these indexes among the NC group and model group, or the miR-133b inhibitor + si-Sp1 group, which were significantly lower in the miR-133b mimic group and si-Sp1 group (P<0.05) and significantly higher on the miR-133b inhibitor group (P<0.05). These indexes in the miR-133b inhibitor + si-Sp1 group was significantly lower compared with the miR-133b inhibitor group (P<0.05). See **Figure 2**.

Cell apoptosis in lung tissues of each group

Compared with the normal group, the other groups had significantly more TUNEL positive cells (P<0.05). Compared with the model group, the number of TUNEL positive cells showed no significant difference in the NC group and the miR-133b inhibitor + si-Sp1 group, while, which in the miR-133b mimic group and the si-Sp1 group were significantly lower, but significantly higher in the miR-133b inhibitor group (P< 0.05). The number of TUNEL positive cells in the miR-133b inhibitor + si-Sp1 group was significantly lower as compared to miR-133b inhibitor groups (all P<0.05). See **Figure 3**.

Expression of Notch-1, Hes-1, and NF-κB P65 mRNA and protein in lung tissues of rats in each group

Compared with the normal group, the mRNA and protein expression levels of Notch-1, Hes-

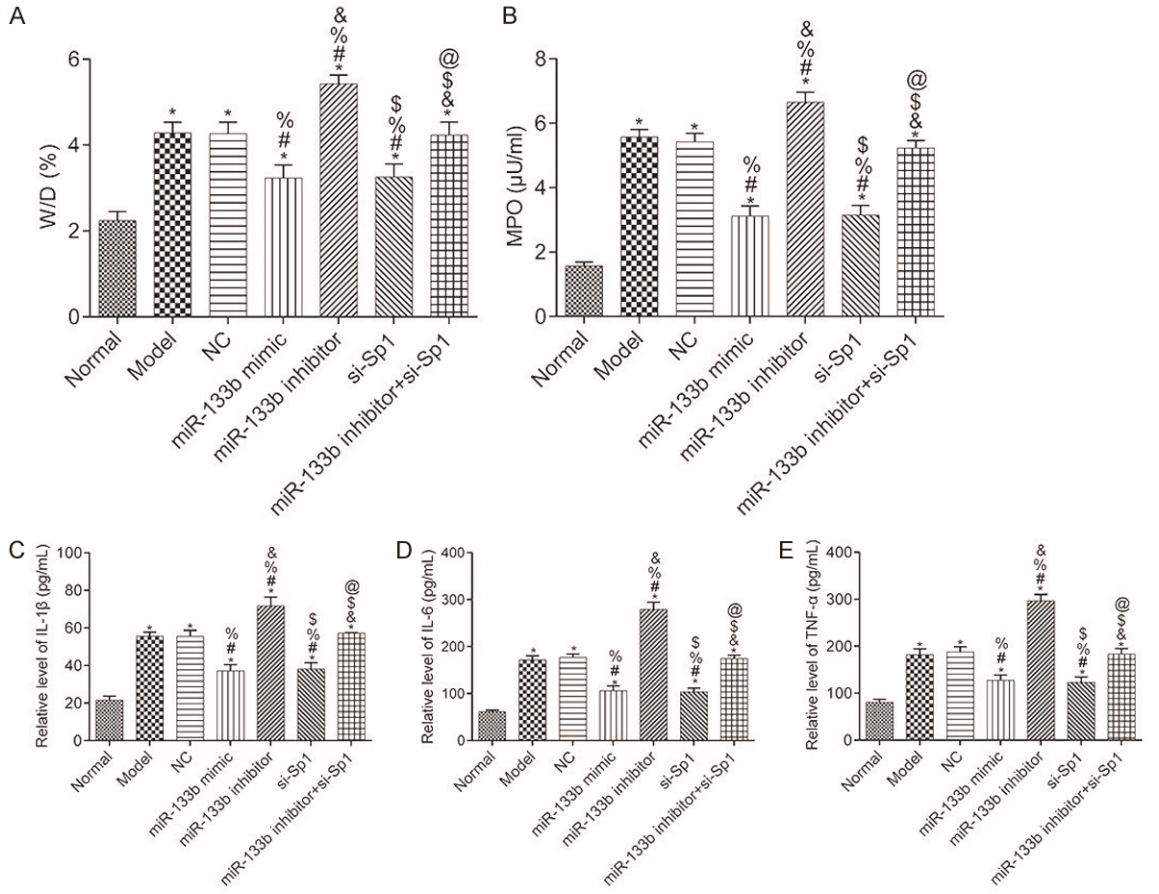

Figure 2. The W/D, MPO activity and IL-1β, and IL-6 and TNF-α levels in each group. A: W/D of lung tissue; B: MPO activity in lung tissue; C: IL-1β level in lung tissue; D: IL-6 level in lung tissue; E: TNF-α level in lung tissue. Compared with normal group, *P<0.05; compared with model group, $^{\#}$P<0.05; compared with NC group, $^{\%}$P<0.05; compared with miR-133b mimic group, $^{\&}$P<0.05; compared with miR-133b inhibitor group, $^{\$}$P<0.05; compared with si-Sp1 group, $^{@}$P<0.05. NC: negative control; W/D: wet/dry weight ratio; MPO: myeloperoxidase; IL: interleukin; TNF: tumor necrosis factor.

1, and NF-κB P65 in other groups were significantly higher (all P<0.05). However, compared with the model group, these indicators showed no significant differences in the NC group or the miR-133b inhibitor + si-Sp1 group, while, which were significantly lower in si-Sp1 group and miR-133b mimic group, but significantly higher in miR-133b inhibitor group (P<0.05). These indicators in miR-133b inhibitor + si-Sp1 group were significantly lower compared with the miR-133b inhibitor group (P<0.05). See **Figure 4**.

Discussion

Without a comprehensive molecular understanding of its pathology, ALI remains a clinical challenge and was difficult to treat directly [20]. Recently, clinical and experimental studies have evaluated reliable markers that may be involved in the diagnosis and prognosis of patient with ALI [21, 22]. Lungs are very susceptible to inflammatory attacks and are the most susceptible extra-pancreatic tissues to be affected due to complications caused by pancreatic injuries. Inflammation promotes the transport of immune cells, rapidly increasing the pro-inflammatory factors by activating multiple inflammatory pathways and releasing tissue-degrading enzymes, which leads to the damage of lung tissues [23]. By studying lung injury caused by acute pancreatitis, factors can be evaluated that cause pancreatic cell damage and distant organ damage. This may help improve the current treatment strategies, reducing morbidity and mortality.

There are 21 Sp1/KLFs genes in humans while in the rat 17 Sp1/KLFs proteins are homologous to human proteins. The Sp1/KLFs family

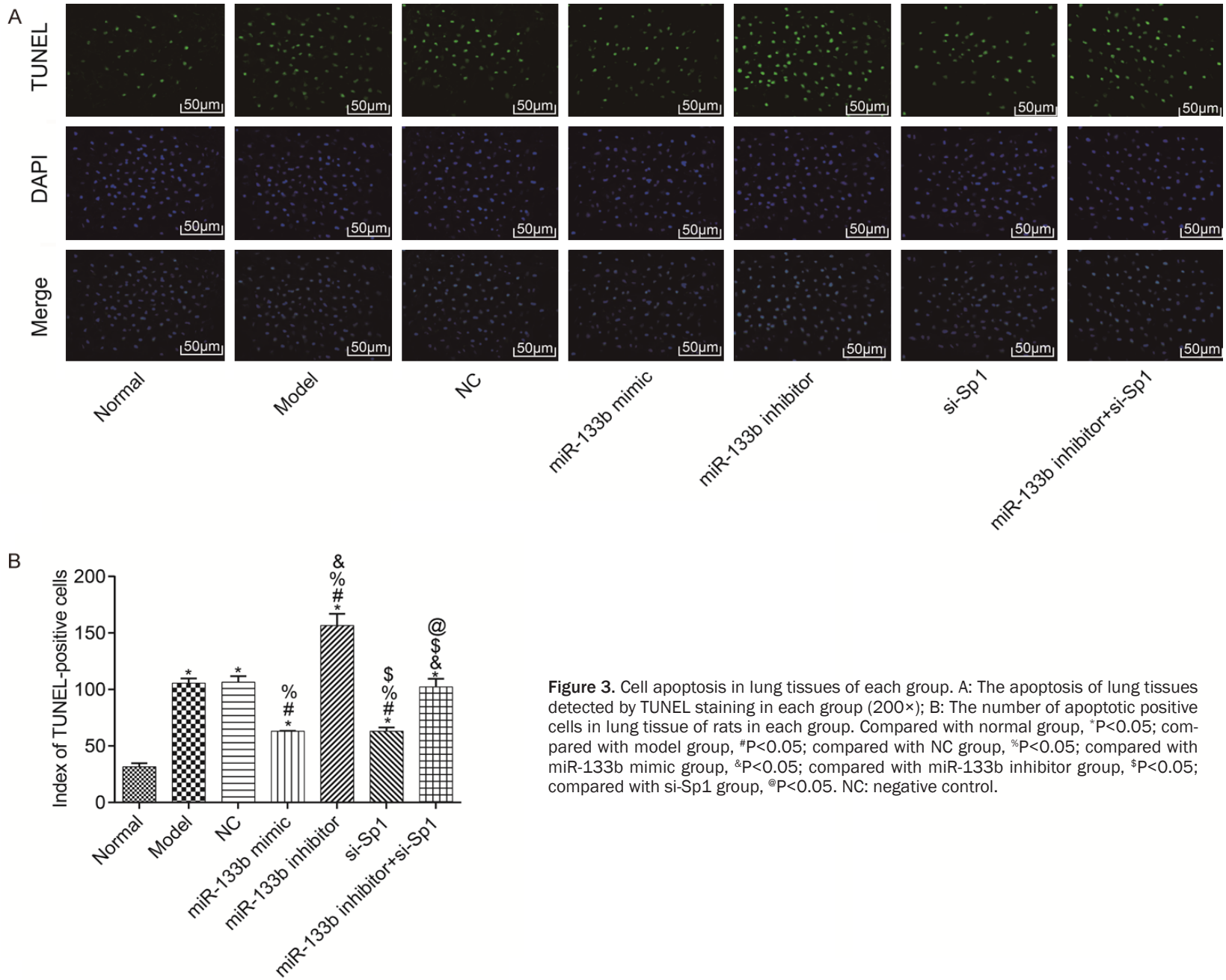

Figure 3. Cell apoptosis in lung tissues of each group. A: The apoptosis of lung tissues detected by TUNEL staining in each group (200×); B: The number of apoptotic positive cells in lung tissue of rats in each group. Compared with normal group, *P<0.05; compared with model group, $^{\#}$P<0.05; compared with NC group, $^{\%}$P<0.05; compared with miR-133b mimic group, $^{\&}$P<0.05; compared with miR-133b inhibitor group, $^{\$}$P<0.05; compared with si-Sp1 group, $^{@}$P<0.05. NC: negative control.

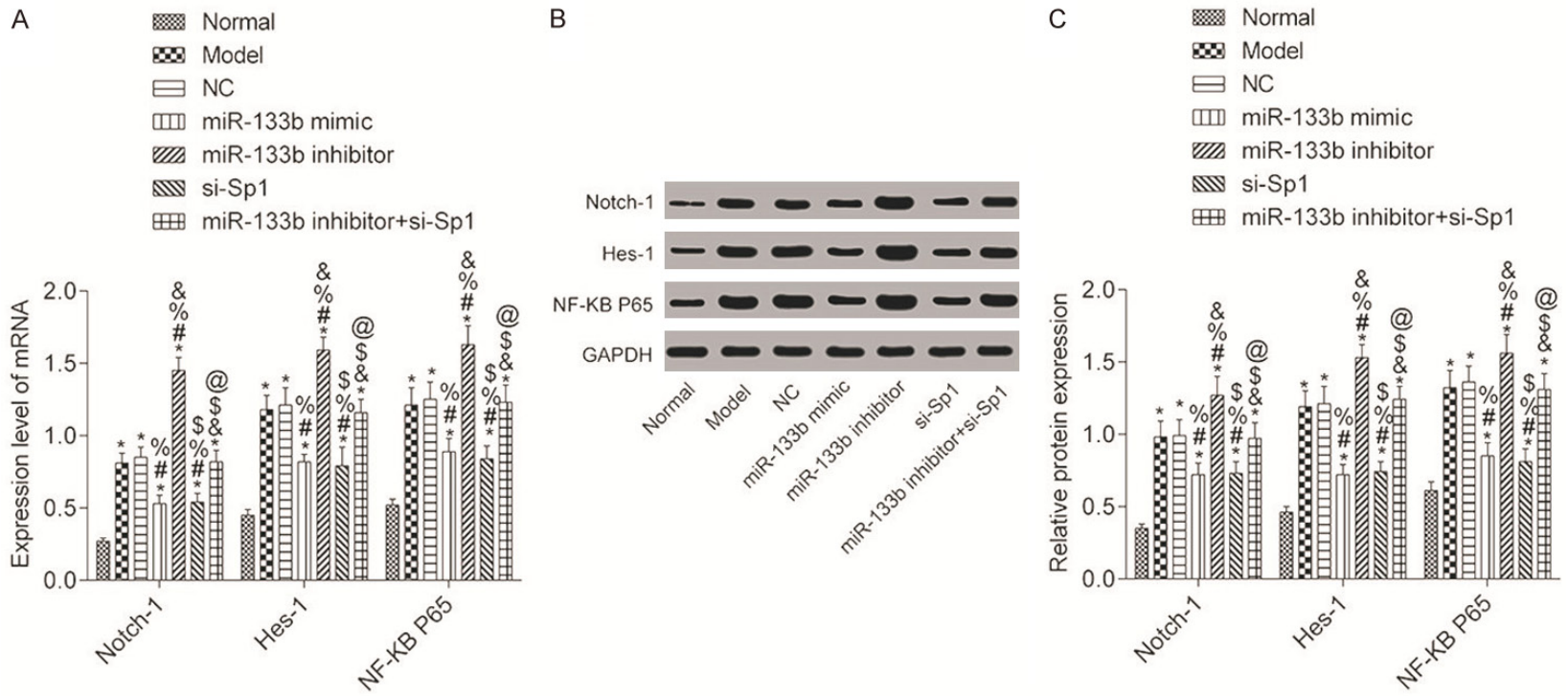

Figure 4. Expression levels of Notch-1, Hes-1, and NF-κB P65 mRNA and protein in each group. A: The mRNA expression levels of Notch-1, Hes-1, and NF-κB P65 in rat lung tissue; B: The protein bands of Notch-1, Hes-1, and NF-κB P65 in rat lung tissue; C: The relative protein expression levels of Notch-1, Hes-1, and NF-κB P65 in rat lung tissue. Compared with normal group, *P<0.05; compared with model group, $^{\#}$P<0.05; compared with NC group, $^{\%}$P<0.05; compared with miR-133b mimic group, $^{\&}$P<0.05; compared with miR-133b inhibitor group, $^{\$}$P<0.05; compared with si-Sp1 group, $^{@}$P<0.05. NC: negative control; NF-κB: nuclear factor kappa-binding.

proteins bind to various GC-rich DNA elements to regulate transcription, cell growth, and control the morphological development [24]. Most of the proteins in the family are involved in regulating growth or development. For example, Sp1 gene knockout in rats lead to developmental delay and death in the early postnatal period [12, 25]. The expression and activity of Sp1 in malignant tumors is higher than that in benign tumors. Sp1 may be involved in the formation of tumors, but it's not clear yet about the role of Sp1 in acute pancreatitis in combination with acute lung injury [26, 27].

Previous studies have shown that the expression of Sp1 is increased in severe acute pancreatitis in rats. The expression of Sp1 can regulate the PI3K/Akt pathway, which then affects the expression of Cystathionine-γ-lyase in peripheral tissues. Cystathionine-γ-lyase is the primary enzyme which produces H2S in peripheral tissues and participates in inflammatory responses [28]. In this study, we injected a Sp1 interference sequence into healthy SD rats and found that lung tissues edema was significantly improved. MPO reduced significantly and inflammatory reactions were significantly decreased, and the cell apoptosis in rat lung tissues was significantly reduced. The expression levels of lung injury-related factors, such as Notch-1, Hes-1, and NF-κB P65, were also significantly reduced. The results showed that the Sp1 interference can inhibit the activation of Notch-1, Hes-1, and NF-κB P65 signaling pathways, thereby reducing inflammation in rat lung tissues in rats with severe acute pancreatitis combined with acute lung injury. Previous studies have reported that Notch-1, Hes-1, and NF-κB P65 are involved in the inhibition of apoptosis of gastric cancer cells and apoptosis inducing and growth inhibition of prostate cancer PC-3 cells [29, 30].

To investigate the upstream regulatory mechanism of Sp1, a prediction analysis using the bioinformatic website was performed. We found that there was a targeting relationship between Sp1 and miR-133b. Till date, downregulation of miR-133b has been observed in a variety of diseases, including Parkinson's disease, rat cerebral hemorrhage, and canine osteosarcoma [31-33]. A previous study has also showned that miR-133b has inhibitory effects in various cases [34]. We suspected that miR-133b may play a role in SAP, complicated with ALI, by targeting Sp1. Thus, we performed the dual luciferase assay and the results confirmed that miR-133b can negatively regulate the Sp1 activity. We also injected miR-133b mimic, miR-133b inhibitor, and miR-133b inhibitor + si-Sp1 vector into rats, respectively. The results showed that the overexpression of miR-133b can improve acute lung injury, which was caused by severe acute pancreatitis in rats. On the contrary, silencing of miR-133b can aggravate the acute lung injury, which can get alleviated when Sp1 expression was inhibited. These results were consistent with our speculation.

For a further confirmation, the study needs to be replicated in a clinical setting. The link between miR-133b and acute pancreatitis combined with acute lung injury has also not been fully explained thus far. Since miR-133b has an inhibitory effect on the Sp1 expression, the molecular mechanism is waiting to be explored. The regulatory role of miR-133b in the disease remains unclear.

In conclusion, we have shown that miR-133b plays a protective role against acute lung injury caused by severe acute pancreatitis by targeting the Sp1 gene. This study further elucidates the pathogenesis of acute pancreatitis combined with acute lung injury, and lays a theoretical foundation for its clinical treatment.

Disclosure of conflict of interest

None.

Address correspondence to: Nan Lin, Department of Emergency, The Affiliated Hospital of Qingdao University, No. 16 Jiangsu Road, Qingdao 266003, Shandong Province, China. Tel: +86-19883237823; Fax: +86-0532-82911283; E-mail: linnan16td@163.com

References

[1] Luo YP, Che W and Zhao MY. Ulinastatin post-treatment attenuates lipopolysaccharide-induced acute lung injury in rats and human alveolar epithelial cells. Int J Mol Med 2017; 39: 297-306.

[2] Owusu L, Xu CM, Chen HL, Liu GL, Zhang GX, Zhang JW, Tang ZK, Sun ZW and Yi X. Gamma-enolase predicts lung damage in severe acute pancreatitis-induced acute lung injury. J Mol Histol 2018; 49: 347-356.

[3] Zhou Y, Xia HM, Zhao L, Mei FC, Li M, You YD, Zhao KL and Wang WX. SB203580 attenuates acute lung injury and inflammation in rats with acute pancreatitis in pregnancy. Inflammopharmacology 2019; 27: 99-107.
[4] Jin YP, Liu LW, Chen BC, Bai YY, Zhang F, Li Q, Lv CQ, Sun HW, Li JJ, Rubby S, Yang LH, Andersson R and Zhou MT. Involvement of the PI3K/Akt/NF-kappaB signaling pathway in the attenuation of severe acute pancreatitis-associated acute lung injury by sedum sarmentosum bunge extract. BioMed Res Int 2017; 2017: 9698410.
[5] Yang ZY, Ji W, Li M, Qi ZD, Huang R, Qu JD, Wang HL and Wang HQ. Protective effect of nimesulide on acute lung injury in mice with severe acute pancreatitis. Am J Transl Res 2019; 11: 6024-6031.
[6] Hong YP, Guo WY, Wang WX, Zhao L, Xiang MW, Mei FC, Abliz A, Hu P, Deng WH and Yu J. 4-phenylbutyric acid attenuates pancreatic beta-cell injury in rats with experimental severe acute pancreatitis. Int J Endocrinol 2016; 2016: 4592346.
[7] Zhao S and Liu MF. Mechanisms of microRNA-mediated gene regulation. Sci China C Life Sci 2009; 52: 1111-6.
[8] Li JY, Liang ZA and Zheng J. MicroRNA-625 serves as a tumor suppressor in non-small cell lung cancer through targeting SOX4. Int J Clin Exp Med 2018; 11: 3225-3234.
[9] Shi N, Deng LH, Chen WW, Zhang XX, Luo RJ, Jin T, Ma Y, Du C, Lin ZQ, Jiang K, Guo J, Yang XN and Xia Q. Is microRNA-127 a novel biomarker for acute pancreatitis with lung injury? Dis Markers 2017; 2017: 1204295.
[10] Theis T, Yoo M, Park CS, Chen J, Kügler S, Gibbs KM and Schachner M. Lentiviral delivery of miR-133b improves functional recovery after spinal cord injury in mice. Mol Neurobiol 2017; 54: 4659-4671.
[11] Kaczynski J, Cook T and Urrutia R. Sp1- and Kruppel-like transcription factors. Genome Biol 2003; 4: 206.
[12] Rao LY, Cui ZG, Niu HY, Qi YL, Yang Z and Lan YH. Reduced Sp1 expression inhibits proliferation and migration of HepG2 cells. Int J Clin Exp Med 2019; 12: 1791-1796.
[13] Black AR, Black JD and Azizkhan-Clifford J. Sp1 and krüppel-like factor family of transcription factors in cell growth regulation and cancer. J Cell Physiol 2001; 188: 143-160.
[14] Wang ZQ, Cai Q, Hu L, He CY, Li JF, Quan ZW, Liu BY, Li C and Zhu ZG. Long noncoding RNA UCA1 induced by SP1 promotes cell proliferation via recruiting EZH2 and activating AKT pathway in gastric cancer. Cell Death Dis 2017; 8: e2839.
[15] Werner L, Berndt U, Paclik D, Danese S, Schirbel A and Sturm A. TNFalpha inhibitors restrict T cell activation and cycling via Notch-1 signalling in inflammatory bowel disease. Gut 2012; 61: 1016-1027.
[16] Kuang SQ, Fang Z, Zweidler-McKay PA, Yang H, Wei Y, Gonzalez-Cervantes EA, Boumber Y and Garcia-Manero G. Epigenetic inactivation of Notch-Hes pathway in human B-cell acute lymphoblastic leukemia. PLoS One 2013; 8: e61807.
[17] Kowalewski C, Kurpios-Pieca D, Rahden-Staron I, Beat Gajewska B and Wozniak K. The potential role of NF-kB activation and synthesis of pro-inflammatory mediators in the pathogenesis of allergic contact dermatitis induced by thiuram. Clin Transl Allergy 2015; 5: 1.
[18] Zhu RT, Zhao YP, Li XB, Bai T, Wang S, Wang WJ and Sun YL. Effects of penehyclidine hydrochloride on severe acute pancreatitis-associated acute lung injury in rats. Biomed Pharmacother 2018; 97: 1689-1693.
[19] Wang Y, Yang Y, Sun JC, Kong QJ, Wang HB and Shi JG. Effect of the adenovirus mediated Wip1 gene on lumbar intervertebral disc degeneration in a rabbit model. Mol Med Rep 2017; 16: 9487-9493.
[20] Chu KE, Fong Y, Wang D, Chen CF and Yeh DY. Pretreatment of a matrix metalloproteases inhibitor and aprotinin attenuated the development of acute pancreatitis-induced lung injury in rat model. Immunobiology 2018; 223: 64-72.
[21] Wang CZ, Gu WT, Zhang YP, Ji YW, Wen Y and Xu X. Nicotine promotes cervical carcinoma cell line HeLa migration and invasion by activating PI3k/Akt/NF-kappaB pathway in vitro. Exp Toxicol Pathol 2017; 69: 402-407.
[22] Wang T. Basic and clinical research progress in acute lung injury/acute respiratory distress syndrome. Infect Int 2018; 7: 38-43.
[23] Yu J, Ni L, Zhang XY, Zhang J, Abdel-Razek O and Wang GR. Surfactant protein D dampens lung injury by suppressing NLRP3 inflammasome activation and NF-kappaB signaling in acute pancreatitis. Shock 2019; 51: 557-568.
[24] Schanton M, Maymo J, Perez-Perez A, Gambino Y, Maskin B, Dueñas JL, Sánchez-Margalet V and Varone C. Sp1 transcription factor is a modulator of estradiol leptin induction in placental cells. Placenta 2017; 57: 152-162.
[25] Tang YF, Yu SY, Liu Y, Zhang JJ, Han L and Xu ZY. MicroRNA-124 controls human vascular smooth muscle cell phenotypic switch via Sp1. Am J Physiol Heart Circ Physiol 2017; 313: H641-H649.
[26] Ling ZX, Liu DC, Zhang GY, Liang Q, Xiang P, Xu Y, Han XH and Tao T. miR-361-5p modulates metabolism and autophagy via the Sp1-medi-

ated regulation of PKM2 in prostate cancer. Oncol Rep 2017; 38: 1621-1628.
[27] Zhao GL, Han CY, Zhang Z, Wang L and Xu J. Increased expression of microRNA-31-5p inhibits cell proliferation, migration, and invasion via regulating Sp1 transcription factor in HepG2 hepatocellular carcinoma cell line. Biochem Biophys Res Commun 2017; 490: 371-377.
[28] Liu Y, Liao RB, Qiang ZR and Zhang C. Pro-inflammatory cytokine-driven PI3K/Akt/Sp1 signalling and H2S production facilitates the pathogenesis of severe acute pancreatitis. Biosci Rep 2017; 37: BSR20160483.
[29] Yao J and Qian C. Over-activated Notch-1 protects gastric carcinoma BGC-823 cells from TNFα-induced apoptosis. Dig Liver Dis 2009; 41: 867-874.
[30] Mukhtar H, Adhami V and Afaq F. Delphinidin induces apoptosis and growth inhibition of prostate cancer PC-3 cells via inhibition of Notch-1 and NF- κβ/PI3κ pathways. Cancer Res 2007; 67.
[31] Zhang X, Yang R, Hu BL, Lu PC, Zhou LL, He ZY, Wu HM and Zhu JH. Reduced circulating levels of miR-433 and miR-133b are potential biomarkers for parkinson's disease. Front Cell Neurosci 2017; 11: 170.
[32] Shen HT, Yao XY, Li HY, Li X, Zhang TJ, Sun Q, Ji CY and Chen G. Role of exosomes derived from miR-133b modified MSCs in an experimental rat model of intracerebral hemorrhage. J Mol Neurosci 2018; 64: 421-430.
[33] Leonardo L, Laura P and Serena BM. miR-1 and miR-133b expression in canine osteosarcoma. Res Vet Sci 2018; 117: 133-137.
[34] Huang B, Jiang XC, Zhang TY, Hu YL, Tabata Y, Chen Z, Pluchino S and Gao JQ. Peptide modified mesenchymal stem cells as targeting delivery system transfected with miR-133b for the treatment of cerebral ischemia. Int J Pharm 2017; 531: 90-100.